Chapter 3

Optoelectronics and Bio Devices on Paper Powered by Solar Cells

António T. Vicente, Andreia Araújo, Diana Gaspar,

Lídia Santos, Ana C. Marques, Manuel J. Mendes,

Luís Pereira, Elvira Fortunato and Rodrigo Martins

Additional information is available at the end of the chapter

http://dx.doi.org/10.5772/66695

Abstract

The employment of printing techniques as cost-effective methods to fabricate low cost, flexible, disposable and sustainable solar cells is intimately dependent on the substrate properties and the adequate electronic devices to be powered by them. Among such devices, there is currently a growing interest in the development of user-oriented and multipurpose systems for intelligent packaging or on-site medical diagnostics, which would greatly benefit from printable solar cells as their energy source for autonomous operation.

This chapter first describes and analyzes different types of cellulose-based substrates for flexible and cost effective optoelectronic and bio devices to be powered by printed solar cells. Cellulose is one of the most promising platforms for green recyclable electronics and it is fully compatible with large-scale printing techniques, although some critical requirements must be addressed. Paper substrates exist in many forms. From common office paper, to packaging cardboard used in the food industry, or nanoscale engineered cellulose (e.g. bacterial cellulose). However, it is the structure and content of paper that determines its end use. Secondly, proof-of-concept of optoelectronic and bio devices produced by inkjet printing are described and show the usefulness of solar cells as a power source or as a chemical reaction initiator for sensors.

Keywords: cellulose, optoelectronic and bio devices, paper characterization, inkjet printing, solar cells on paper substrates

1. Introduction

1.1. Printing technology

The e-market for flexible and printed large-area electronics is rapidly growing and it is expected to become a $69 billion market in the next 10 years [1]. The growth is manly supported by the organic light-emitting diodes (OLEDs) and conductive ink industries. Nevertheless, as technology emerges from R&D, new market opportunities with huge growth potential will appear. Two potential markets are the food and health. These industries are facing a paradigm shift as society demands more regulation, quality control, and smart systems to improve life quality while being environmentally friendly and allowing continuous user interface. Printed electronics can be the key to address such demands by imparting products with solutions to acquire, store, and transfer data, communicate and carry out logic functions to take decisions, where recyclability and low cost are key vectors [2].

Printing technologies enable electronics to be readily integrated as a part of other printed media by processing them in the same press. This renders possible low cost products such as radio frequency identification (RFID), intelligent packaging, food quality control devices, or disposable diagnostic kits. Functionality and performance of printed electronics are not intended to compete with silicon-based electronics, nevertheless, mass-printing methods offers economic advantages for large-scale production of appropriate products. Printing technology is highly customizable, it is compatible with the preferable fabrication method in industry—the roll-to-roll (R2R)—does not require large vacuum chambers and has lower capital investment costs when compared with other production methods. It is estimated that a printed electronics facility will cost 100 times less than a conventional silicon electronics plant.

There are various printing techniques, such as inkjet, screen, flexography, gravure, or offset printing, and their features expand the range of applications. The selection of the printing method is dictated either by the requirements concerning printed films or the level of printing system complexity. In the field of electronics, printing techniques are used to apply coatings, to deposit precise patterning, or even to develop microstructures [3]. Inkjet printing patterns material by expelling from the nozzle one picoliter droplet of ink at a time, as the printhead moves over the substrate. It is a method suitable for low-viscosity inks (1–20 cP). Screen printing is a highly versatile technique given its simplicity and reproducibility. To print, a squeegee transfers the ink through a patterned screen onto a substrate. Gravure (or rotogravure), flexography, and offset printing use a rotary printing press. Gravure printing is the most popular process for flexible packaging manufacturing and it consists in applying ink to an engraved cylinder, which is then transferred (directly, or indirectly through a transfer roll) to the substrate. The flexographic technique prints on flexible substrates by ink transfer (with low viscosity, 50–500 cP) from a laser-etched flexible relief plate. Offset printing is the preferable method for newspaper printing. It works on the principle of oil and water repulsion. A plate is damped first in water (nonimage area) and then ink (image area); the ink adheres to the print area, then it is transferred to a rubber blanket and from it to the paper.

http://dx.doi.org/10.5772/66695

1.2. Paper electronics and its thermal management

Electronic devices fabricated on plastics are currently a booming field of research [4–10]. Polyethylene naphthalate (PEN) and polyethylene terephthalate (PET) foils are the most used substrates for printed electronics, because of their high smoothness and good electrical and barrier properties [11, 12]. Physical properties, such as roughness, absorptive capacity, temperature resistance, and flexibility, are also critical. PET foil meets most of these requirements but PEN is also an interesting option given its greater dimensional and thermal stability [13]. PI (polyimide, named Kapton) is another widely used polymeric substrate for flexible thin film solar cells, due to its remarkable chemical and thermal robustness (withstands up to 300–400°C) and bendability [14]. Nonetheless, for low-cost devices, the price of these synthetized materials can be high and its use is ecologically questionable, since they are not biodegradable and are produced from oil-based raw materials.

On the other hand, paper is potentially useful for some specific applications and markets, such as those already mentioned of intelligent packaging and diagnostic kits [15], where low cost (€0.001 dm^{-2} compared with €25 dm^{-2} for silicon or €1–10 dm^{-2} for polymer substrates) and sustainability are highly desirable. Cellulose is the most abundant natural biopolymer on earth, which is recyclable, biodegradable, as well as nontoxic. It is a carbohydrate polymer made up of repeating β-D-glucopyranose units and consists of three hydroxyl groups per anhydroglucose unit (AGU), giving the cellulose molecule a high degree of functionality. The knowledge of the molecular structure of cellulose is of prime importance as it explains the characteristic properties of cellulose, such as hydrophilicity, chirality, biodegradability, and high functionality [16], which are key factors as far as device feasibility is concerned.

Cellulose fibers have remarkable properties, in particular their thermal and mechanical dimensional stability when compared to plastics, for instance. This is of particular interest if alignment is required when printing different functional materials on top of paper substrates. Paper is commonly used as a dielectric for capacitors [17] and supercapacitors [18], as permeable membranes in liquid electrolyte batteries [19, 20], or just as the physical support of energy storage devices [21], as an organic thin film transistor (OTFTs) [22], printed sensors, and RFID tags [23], printed batteries [24], inorganic powder electroluminescence devices [25], foldable printed circuit boards [26], oxide TFTs [27], and flexible low-voltage electric double-layer TFTs [28].

Many end-user devices will then require power sources, either to display information, integration with other devices, or simply to improve their processing capabilities and complexity. Though recent advances in paper batteries aim to suppress those power requirements, full autonomy can only be achieved by coupling a power generator, such as a solar cell. Hence, one can envision the interconnection of several paper functionalities, to accomplish self-sufficient electronic intelligent paper, or enable disposable sensors of complex laboratory functions (lab-on-chip), as seen in **Figure 1**.

Nevertheless, the substrate requirements for printed electronics are much more demanding than for image printing, hence cellulose substrates have numerous challenges. Homogenous,

pinhole-free layers are essential to ensure the desired functionality of the deposited layers, and conventional paper substrates present limitations such as roughness on a length scale of micrometers, porosity, and hydrophilic characteristics. Research has focused on modifying papers for the specific requirements of printed electronics and the paper surface can be modified in a thermal-mechanical manner (i.e., calendered or coated). Normally, the coatings consist of pigments and binders in an aqueous dispersion. However, rendering paper a suitable substrate for active materials can be expensive and may require materials and techniques that are neither cheap nor environmentally friendly [29, 30], diluting the advantage of using a paper substrate over plastic foils for mass production. Moreover, there are reports of chemical interaction/reaction with the selected coating, which degrades the electrical performance of the organic functional layer, as observed when printing PEDOT:PSS on paper [31]. This means that it is difficult to develop a coating, which is chemically compatible with all the inks required to print electronic devices based on organic materials. Another important aspect to consider is the process temperature of the functional materials being deposited on paper which must stay below 200°C in order to avoid cellulose degradation [32].

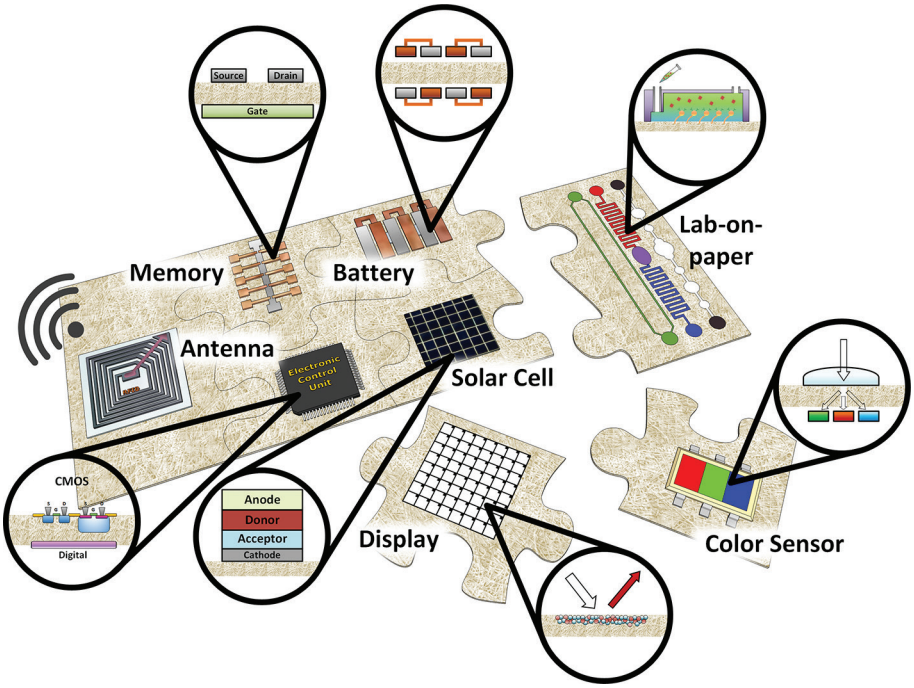

Figure 1. Concept of the multiple integration of devices built with or on paper to perform complex functions. A solar cell coupled with a battery assures full autonomy to a device that requires energy to perform logic operations at the electronic control unit (CMOS), given the signals received from the sensor unit, and then distributes the processed information to be saved in a papermemory or transmitted by an RFID antenna to another device. Other devices/functions can be added according to the final application, such as a display to visually convey messages to the user, or a lab-on-paper diagnostic device.

http://dx.doi.org/10.5772/66695

Though not always using printing deposition techniques, recently, some attempts envisaged to use paper in electronic applications to explore its potential as substrate for low-cost flexible devices [33, 34]. These can complement the functional inks, but their electric performance and stability hardly meet the requirements without specific deposition conditions and encapsulation [29, 35].

Electronics on paper has been investigated since the 1960s, when TFTs were deposited on paper substrates on a roll inside a vacuum chamber [36, 37]. The envisioned applications were flexible circuits for credit cards, electric sensors, toys, and hobby kits; but without any industrial or commercial success since the technology appeared during the boom of the silicon-based CMOS devices that fueled a revolution in the so-called information, communication and telecommunication (ICT) fields. Since then, research on paper-based field effect transistors (FETs) [38–42] has shown that paper could be used as an active component (dielectric). This has established a new approach to the challenge of *paper electronics*, where performance and stability issues are addressed using inorganic semiconductors, not requiring any special paper surface preparation nor device passivation. Likewise, devices with oxide functional materials can also benefit from the fact that cellulose is chemically more compatible with oxides than with many organic semiconductors [43], they bind properly at low temperatures and the natural porosity of paper can be explored in practical applications. Cellulose also provides a high surface area matrix for memories and sensors, for instance, as well as the capacity of electronic charge accumulation at the fiber surface for the integration of electronic components, as demonstrated by our recent research activity [41].

So far, some of the materials and techniques proposed to build electronic devices on paper are assumed to be compatible with low temperature processing and printing deposition. However, there are no reports yet of fully printed devices on paper that are 100% compatible with roll-to-roll processing. Thus, the solution for this challenge is not only the development of materials that can be printed at low temperatures but also to assure that their energy consumption is not high, so that the power sources to be used (solar cells, primary green batteries, and RF energy harvesting) can efficiently meet the energy needs of the device. The integration of multiple fabrication techniques can also maximize the device performance.

When developing electrical circuits, thermal and power dissipation issues, when a large number of electronic circuits/devices are integrated on an area of square millimeters, are another concern, particularly when using organic inks given their sensibility to temperature. Here, the supply voltage used, the overall current passing through the circuit, and the operating frequencies of such circuits are key factors. Resistors along the circuit are the main source of the heat generated and it corresponds to a bottleneck that forces the use of local heat sinks for enhanced dissipation. To overcome this limitation, paper electronics may not target complex and highly demanding applications but rather niche of low power and low frequency applications, where expected power generation remains very low. For instance, a reasonable target for printed paper electronics is to have no more than 10–50 transistors per cm^2, also because the integration density on paper is driven by the resolution of the printing/depositing processes (tens of microns), which are far lower than the traditional photolithography techniques used in the silicon microelectronic field (tens of nanometers).

Finally, contrary to plastic substrates, paper exhibits high dimensional stability over temperature, which is advantageous for electronic components by not introducing complex thermal parasitic effects in the electronic devices' behavior. For example, an optically transparent paper made of cellulose nanofibers has a coefficient of thermal expansion (CTE) of <8.5 ppm [44], which is much lower than plastic (PEN: 18–20 ppm; PET: 22–25 ppm). Besides, paper can also endure annealing cycles at 200°C for short time periods without any noticeable change in physical characteristics.

1.3. Solar-powered photovoltaic paper

The present development of photovoltaic (PV) devices allows the fabrication of solar cells on a wide variety of low-cost recyclable and disposable substrates such as paper, thereby extending PV, coupled with batteries, to a broad range of consumer-oriented portable applications where autonomous energy harvesting is needed (e.g., wearable PV, solar-powered intelligent packaging, internet-of-things systems).

Two main technological challenges can be identified in the field of PV on paper: (1) the requirement of solar cell (SC) fabrication processes employing low temperatures (below 150°C) and (2) the pronounced surface roughness of the fibrous paper structure, which can create defects in the cell layers and consequently deteriorate their electrical conduction. Such challenges are more relevant for inorganic (e.g., silicon, chalcopyrites, kesterites) based solar cells (given the high temperature, between 200°C and 300°C, typically used in the PECVD deposition of thin film silicon devices) and less crucial for organic or dye-sensitized–based cells as these devices can be processed without high temperature and by nonvacuum methods (e.g., screen printing, doctor blading, spin coating, spray deposition, electrochemical deposition) and their performance is more tolerant to the defect density [45], but at the same time more sensible to the substrate chemistry. Regardless of their lower environmental stability and power conversion efficiency, these PV materials are still considered the most suitable option for the development of printable solar cells [46] given their minimum detrimental impact on the cellulose substrate. Barr et al. successfully integrated solar cells directly onto as-purchased papers without pretreatment to fill interfiber spaces. The paper PV arrays produced more than 50 V, enough to power common electronic displays under ambient indoor lighting, and can be flexed and folded without loss of function [47].

Thin film hydrogenated amorphous silicon solar cells have been already successfully implemented on distinct types of cellulose-based substrates, such as liquid-packaging cardboard [48] and printing paper [49] with sunlight-to-electricity conversion efficiencies of 3–4%. This was attained by developing appropriate low-temperature PECVD processes and by coating the paper surface with a hydrophilic mesoporous layer. Such layer can, not only withstand the cells production temperature, but also provide adequate paper sealing and surface finishing for the cell's layers deposition. A key procedure performed in such works is the continuous monitoring of the substances released from the paper substrates during the cell deposition by mass spectrometry, which allows adapting the fabrication processes to mitigate any contamination from the substrate. Transfer printing or lamination is another class of methods that can also be adapted to inorganic and thin film solar cells. With these methods the cell layers are first deposited on a donor substrate, which is compatible with the optimal fabrication condi-

http://dx.doi.org/10.5772/66695

tions (usually high temperature and under vacuum), then they are detached from the original substrate and transferred to another receiver substrate (e.g., a flexible low-temperature tolerant platform such as paper) [50, 51]. For instance, a transfer printing method is applied in the work of Lee et al. where GaAs photovoltaic modules are transferred to a prestrained, structured substrate of PDMS with a power conversion efficiency (PCE) ≥20% [52]. A similar method was employed on cellulose nanocrystal (CNC) substrates to fabricate SCs with a PCE of 4.0% [53], and 5.9% on optimized transparent paper [54].

Another key point to take into account in the fabrication of solar cells on flexible substrates, such as paper, is the front illuminated contact. This transparent contact must be of particular high performance to realize efficient large-area (centimeters scale) devices. Such contact is conventionally composed of a transparent conductive metal oxide (TCO), but research on alternative and inexpensive methods is essential. Examples of such alternatives are metallic networks engineered by soft lithography, such as colloidal lithography or nano-imprint; and the production of conductive transparent paper, for instance by using cellulose nanofibers and printing silver nanowires[55]. The colloidal lithography approach has allowed engineering innovative ultrathin electrodes with a honeycomb lattice structure [56], known as micromesh electrodes (MMEs) [57, 58], which already shows transmittance (T ~91% in visible range) and sheet resistance (Rs ~6.2 Ohm/square) better than the state-of-the-art ITO (Rs ~10 Ohm/square and T ~90%) [59]. Besides, MMEs on flexible polyimide substrates were shown to remain invariant after 1000 cycles of repeat bending to a 2 mm bending radius [64]. As for the conductive paper using cellulose nanofibers and silver nanowires, it presents an optical transparency and electrical conductivity as high as those of ITO glass. The SCs fabricated on such conductive paper exhibited a PCE of 3.2% and generate electrical power even under and after folding.

Lastly, despite all the efforts on solar cell material optimization, efficiencies achieved so far are still considerably below the state-of-the-art (11–13%) on rigid (usually glass) substrates. Advanced light trapping methods employing wavelength-sized photonic structures are regarded as one of the most promising strategy to boost light absorption, allowing thickness reduction while keeping high efficiency [14, 45, 60, 61]. Optically thicker but physically thinner devices imply cheaper and faster fabrication, light-weight and improved flexibility which enables roll-to-roll fabrication on the flexible paper substrates. Besides, thickness reduction can lead to higher open-circuit voltages (and consequently efficiencies) due to lower bulk charge-carrier recombination [62, 63].

2. Cellulose substrates for electronic devices: characterization techniques and properties

Despite the technological applications of paper, there are few contributions regarding cellulose-based substrates characterization, and its applicability in electronic devices. The device and material requirements often limit the choice of the paper substrate, thus a complete understanding of its characteristics, namely, surface morphology, roughness, thermal sta-

bility, flexibility, mechanical strength, and hydrophobicity, is essential to assure the proper device operation.

Paper substrates are generally classified based on their weight or *grammage* and can be divided in three categories, following the suggestion of Tobjörk and Österbacka [43]: Light paper, whose *grammage* is in the range of 12–30 g m^{-2}, or for thickness below 75 μm; standard paper, such as office paper, which is around 80 g m^{-2} and 100 μm thick; and cardboard (or paperboard), when the *grammage* exceeds 200–800 g m^{-2}, or when the thickness is above 300 μm:

- **Light paper**. In this category, one can place two cellulose substrates that are attracting much attention in the recent years: bacterial cellulose (BC) and nanocrystalline cellulose (NCC).

Bacterial cellulose is a bacteria-produced biopolymer composed of ultrafine nanofibers (<100 nm wide); the major perks of this material, comparing to the nanocellulose obtained from wood, is its purity and crystallinity since it is free of lignin, hemicellulose, and other components present in the vegetable cellulose [64–66]. This material can be obtained from several cellulose-producing bacteria, such as *Gluconacetobacter genus, Agrobacterium tumefaciens*, bacteria of the genera *Pseudomonas*, among others; the cellulose is produced extracellularly since the bacteria excretes the cellulose into an aqueous culture medium, of low molecular weight sugars, directly as nanofibers, which form a porous three-dimensional nanocellulose mesh structure [67–69]. The grown layer is then harvested from the medium, cut and dried.

Nanocrystalline cellulose can be obtained primarily from cotton. NCC membranes are prepared through the acid hydrolysis of cellulose process [70]. Cotton is one of the purest cellulose sources, given its higher amount of cellulose (90 wt%), when compared with other vegetal sources that usually contain a mass fraction between 50 wt% (wood) and 80 wt% (flax or hemp) [40, 67, 71]. These membranes are highly transparent, lightweight, and have a smooth surface [40]. The flexibility of some NCC papers and the unique optical properties of nanocrystalline cellulose open a wide range of cost-efficient applications, for instance, smart labels, RFID, smart packaging, or even as support for bio-applications.

- **Standard paper**. There are countless types of paper in this category. The varieties here discussed are the most relevant for this chapter: commercial office paper (COP), raw paper (RP), the *Whatman* filter papers (WFP1 and 4), and the vegetable papers – parchment paper (PP) and tracing paper (TP), with thickness of 60, 135, 180, 205, 52, and 80 μm, respectively. The commercial office paper presented here is an 80 g m^{-2} *grammage* paper made from the Portuguese paper manufacturer the *Navigator* company. Raw paper (63 g m^{-2}) is fabricated by *Felix Schoeller Group*. The W*hatman* filter papers are used worldwide for chromatography and are a registered trademark of *GE Healthcare*. WFP1 and WFP4 *grammage* is 88 and 96 g m^{-2}, respectively. Parchment paper (41 g m^{-2}) is commonly used in baking as a disposable nonstick surface and the tracing paper studied here, with a *grammage* of 90 g m^{-2}, was provided by *Canson*, a manufacturer of fine art paper and is specially adapted to technical drawing.
- **Cardboard**. For this category, the paper studied is called liquid packaging cardboard (LPC) and it is produced by the Finnish company *Stora Enso* [72]. LPC is an aseptic and biodegradable

material widely used in the food packaging and beverage industry throughout the world. This material comprises three layers: the pressed cellulose fibers (cardboard, 240 g m^{-2}), an adhesive layer of low density polyethylene (LDPE, 12 g m^{-2}), and the aluminum sheet (6–7 mm). One major particularity is its robustness to withstand harsh environments, as evidenced by its use as substrate for solar cell deposited by plasma-enhanced chemical vapor deposition (PECVD) [48] and as an efficient surface-enhanced Raman spectroscopy (SERS) platform supporting metal nanoparticles arrays fabricated through thin film annealing [73].

Based on this classification, the following sections present a comprehensive characterization overview and comparison between paper samples of each category.

The assessment of the surface morphology of cellulose substrates can be achieved by scanning electron microscopy (SEM) [39], backed by three-dimensional (3D) profilometry [74] and AFM [38], to evaluate the paper surface, dimension of fibers, thickness, and porosity. Other techniques, such as X-ray diffraction (XRD) [40, 41], differential scanning calorimetry (DSC), thermogravimetric analysis measurements (TGA) [40, 41], and Fourier transform infrared (FTIR) spectroscopy [75, 76], provide information regarding the paper structure and contents. This information in turn can help to understand the optical properties (such as transmittance and haze factor), studied by spectrophotometry [40], or the electrical properties of the cellulose fibers and overall electrical behavior of the paper material. One method to study the electrical properties of cellulose is the fabrication of different transistors (with and on paper) [38–41, 74] and its analysis by impedance spectroscopy [38, 40, 41, 74].

2.1. Light paper

The X-ray diffraction (XRD) diffractogram (**Figure 2a**) provides information regarding the crystallinity index and crystallite size. Bacterial cellulose (BC) and cotton-based nanocrystalline cellulose (NCC) show the presence of characteristic cellulose type I, also defined as native cellulose, given the characteristic peaks at 2θ = 14.7°, 16.9° and 22.9° for BC and 14.7°, 16.8° and 22.7° for NCC. These cellulose type I peaks correspond to the $1\bar{1}0$, 110, and 002 crystallographic planes, respectively. The XRD patterns were collected from 10° to 90° (2θ), with a scanning step size of 0.016°, with a monochromatic CuKα radiation source (wavelength 1.540598 Å). The crystallinity index, I_C, was determined using the method proposed by Segal et al. [77]:

$$I_C = \frac{(I_{(002)} - I_{(am)})}{I_{(002)}} \times 100 \quad (1)$$

where $I_{(002)}$ is the maximum intensity of the diffraction of the (002) lattice peak, taken at a 2θ angle between 21° and 23°, and $I_{(am)}$ is the intensity of the diffraction of the amorphous regions, taken at the minimum on a 2θ angle range between 18° and 20° [40, 41].

The inexistence of lignin and hemicellulose in BC leads to a high crystallinity index (~92%) and a crystallite average size of 5.7 nm, higher than NCC which lies around 80% and has a crystallite average size of 7 nm.

Attenuated total reflectance-Fourier-transformed infrared (FTIR-ATR) spectroscopy provides information regarding the chemical species, chemical bonding state of cellulose, and to infer on the water content. Measurements were recorded using an attenuated total reflectance (ATR) sampling accessory (Smart iTR) with the following conditions: incident angle of 45°; 4000–650 cm^{-1} range; 4 cm^{-1} resolution; 32 scans; 20°C. The FTIR-ATR spectrum (**Figure 2b**) of BC and NCC resembles that typically obtained for plant-based cellulose and depicts the characteristic cellulose absorption peaks, i.e., hydrogen-bonded OH stretching at 3400 cm^{-1}, C–H and C–O stretching vibrations, 2900 and 1060 cm^{-1}, respectively. The O–H bending vibration assigned to the absorbed water is also observed with the presence of a peak at 1640 cm^{-1} [40].

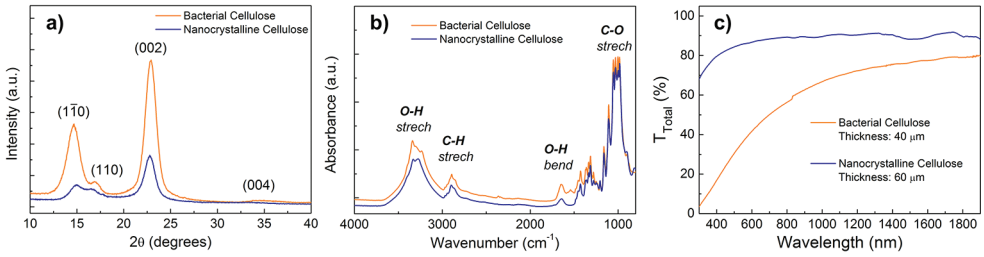

Figure 2. (a) XRD diffractogram of bacterial cellulose (BC) and cotton-based nanocrystalline cellulose (NCC) dried membranes; (b) FTIR spectrum of BC and NCC dried membranes; (c) total transmittance.

The BC membranes have a smooth structure of long entangled filaments of extruded cellulose fibrils with an average width of 20–100 nm (**Figure 3a**) and a surface *RMS* roughness in the order of 60 nm [68, 69, 78]. As for NCC, one can observe a smooth and compact morphology (**Figure 3b**) and also a needle-like structure in the cross-section inset.

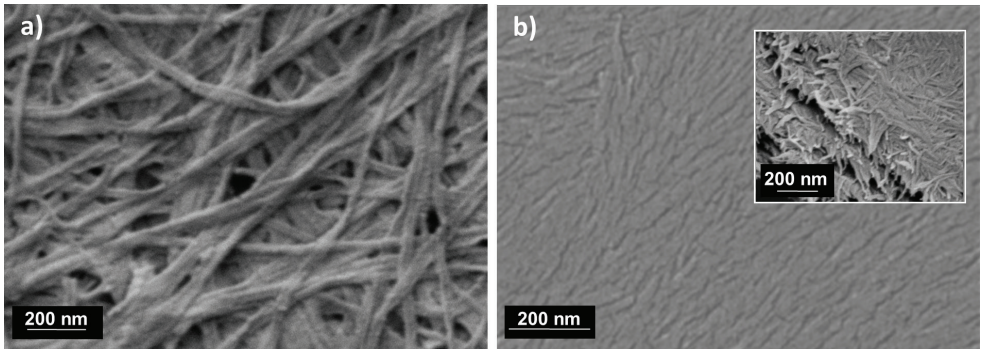

Figure 3. SEM micrograph of the surface morphology of (a) bacterial cellulose and (b) nanocrystalline cellulose membranes (NCC) produced by evaporation and the corresponding cross section (inset). Adapted from Gaspar et al. [40], with permission from IOP Publishing.

http://dx.doi.org/10.5772/66695

The low porosity, roughness in the order of nanometers, and high compactness of the cellulose fibers give these paper substrates a high contact angle (~95°C, accessed through 1 μL of deionized water droplet), which translates in a significant hydrophobicity that is beneficial to microfluidic devices [79], self-cleaning and to prevent the negative effects that the absorption of water can have on electronics devices.

2.2. Standard paper

The SEM micrographs in **Figure 4** show the morphology of the paper samples. COP has a high-density structure of intertwined cellulose fibers, with different shapes and sizes (some wider than 20 μm) and also calcium carbonate agglomerates. RP presents a similar structure and fibril size dispersion, without the presence of calcium carbonate agglomerates. As for the morphology of *Whatman* filter papers (WFP1 and 4), one can observe wide fibers (>20 μm) embedded in a matrix of small ones (<5 μm), whose concentration can be correlated to the intended filter permeability (**Figure 4c** and **d**). Both COP and RP have low porosity and high hydrophobicity (water-contact angle around 100°) when compared to WFP1 and 4 samples, which have a water-contact angle of <10°. The samples with the smoothest, more uniform, and compact surfaces are from parchment (PP) and tracing paper (TP), where the high concentration of small size fibers completely fills the gaps and surface between the larger fibers. The SEM for the PP samples (**Figure 4e**) shows a similar matrix structure of large and small fibers, with dimensions that can exceed 40 μm in width, embedded in a matrix of small ones (<5 μm) but the smoothest and most homogeneous surface is the TP substrate (**Figure 4f**).

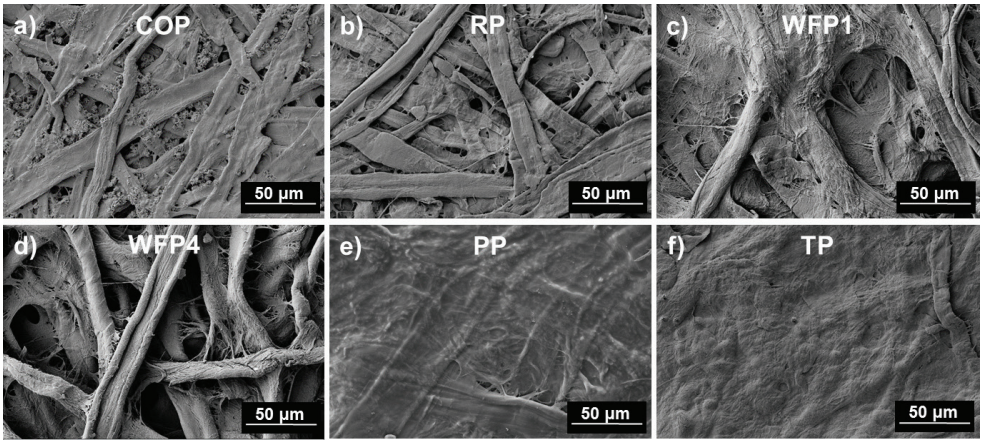

Figure 4. SEM micrographs of the six paper samples: (a) Commercial office paper (CPP), (b) raw paper (RP), (c) *Whatman* filter paper sample 1 (WFP1), (d) *Whatman* filter paper sample 4 (WFP4), (e) parchment paper (PP), and (f) tracing paper (TP).

Figure 5 gathers the 3D profilometry scans of the different paper substrates. As expected, given the fibers' width, the WFP1 and 4 have the surface with the highest root mean square (RMS), exceeding 12 µm. On the opposite side, the TP has the smoothest surface with *RMS* ~4 µm, while COP and RP have similar and slightly higher values of RMS (~5 µm). The COP paper is optimized for printing and therefore has a lower porosity and higher hydrophobicity (water contact angle of 101°) when compared to WFP (water contact angle of <10°), which is hydrophilic in nature, given the dimension of its fibers and high porosity. The high concentration of small size fibers, compactness, and smooth surface of the vegetable papers, PP and TP, also lead to high hydrophobicity (water contact angle of 124° and 95°, respectively).

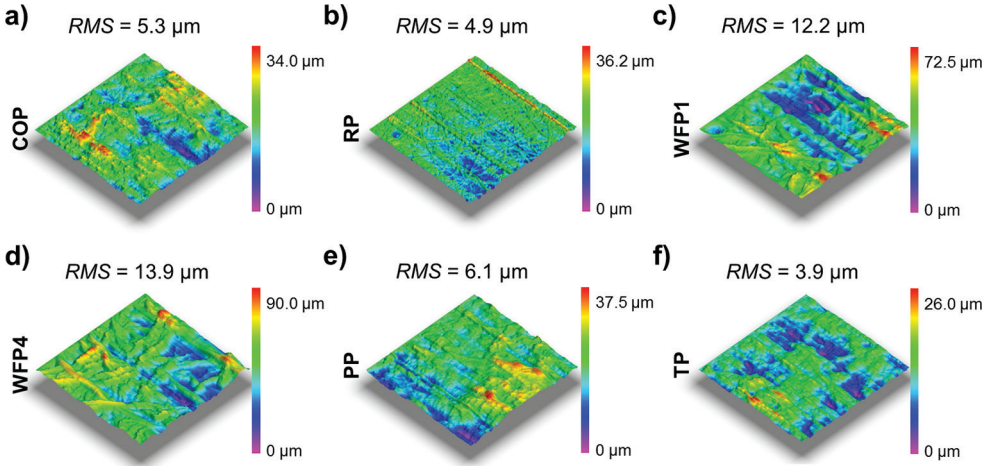

Figure 5. 3D profilometer on a 0.5 × 0.5 mm area of the six paper samples: shown in Figure 4: (a) CPP, (b) RP, (c) WFP1, (d) WFP4, (e) PP, and (f) TP.

The water content and its affinity to the paper substrate also plays an important role as a plasticizer or softening agent, thus influencing paper properties such as flexibility, elasticity, strength, and rigidity, which should be adjusted not only to the fabrication process, but also to the ink impregnation and overall printing quality. A low moisture content give rise to a hard and brittle paper, while a water content too high leads to creasing, delayed ink drying, and poor finish [80].

The analysis of XRD diffraction (**Figure 6a**) highlights the referred differences between COP and the other paper substrates. Besides the common $1\bar{1}0$, 110, and 200 crystallographic planes (respectively at $2\theta = 14.7°$, 16.8°, and 22.7°) associated to semicrystalline cellulose type I (also referred to as native cellulose), the XRD of COP reveals intense peaks between 28° and 50° related to the presence of calcium carbonate ($CaCO_3$) [41, 81]. Calcium carbonate and clay are typically present in paper manufacturing, either from pigments that are commonly used in papermaking or the water mineral content.

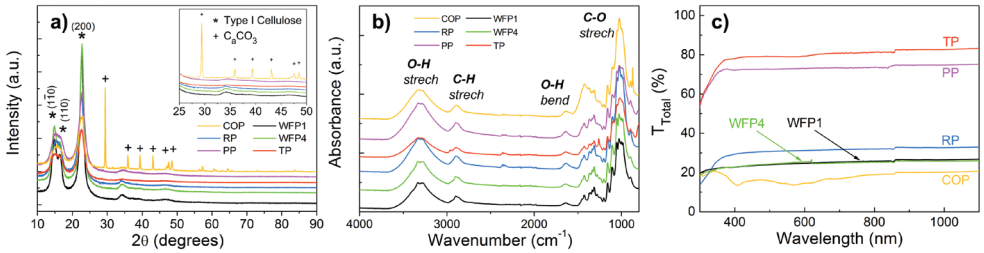

Figure 6. (a) XRD diffractogram of the different papers analyzed in Figures 4 and 5. All paper substrates present the 1$\bar{1}$0, (110), and (002) diffraction peaks of cellulose I (native cellulose). COP also shows intense peaks associated with the presence of $CaCO_3$; (b) FTIR spectrum; (c) total transmittance as a function of wavelength.

In the FTIR-ATR spectra (**Figure 6b**), all samples reveal the bands associated to cellulose, such as OH, C–H, and C–O stretching bands, at 3400, 2900, and 1060 cm^{-1}, respectively. It is also observed a peak at 1640 cm^{-1} for the O–H bending vibration which corresponds to the absorbed water [40]. The 3600–3100 cm^{-1} broad band in the region provides information regarding the hydrogen bonds. The peaks from amorphous cellulose are sharper and have lower intensity, which can be correlated with the scission of the intra- and intermolecular hydrogen bonds [75]. Tracing paper is the sample with the most distinctive and low intensity OH stretch band.

Transmittance can also be an important characteristic of paper devices, for example, in OLEDs; the large optical haze is attractive for organic solar cells or in paper touchscreens to eliminate glare under direct light [44]. The total transmittance spectra of the different paper substrates are shown in **Figure 6c**. Tracing and parchment paper are the most translucid, although there is always a fraction of light that is transmitted regardless of the paper substrate. Scattered light is the main component of transmitted light, which translates in a high haze factor.

Information regarding thermal stability can be obtained by thermogravimetry and differential scanning calorimetry (TG-DSC) analysis (~7.5 mg of sample mass, heated at atmospheric pressure, from 25°C to 550°C with a heating rate of 5°C min^{-1}). Results show an initial weight loss (<10%), at temperatures close to 100°C, which corresponds to the desorption of free water from the cellulose fibers. Thermal degradation of cellulose, by depolymerization and the formation and evaporation of levoglucosan, or oxidative decomposition, occurs for temperatures above 300°C and is followed by a weight loss above 70%.

2.3. Cardboard

The liquid packaging cardboard characterization by SEM and 3D profilometry (**Figure 7**) reveals a continuous and crack-free aluminum foil, shaped to the cardboard roughness (*RMS* ~6 μm). As for TG-DSC analysis, published elsewhere [48], there are two endothermic peaks. The first peak, detected at 99.3°C with a weight loss of 6.6%, is related to the release of free water, and the second peak, at 353°C with weight loss of weight loss of 57.7%, is linked to

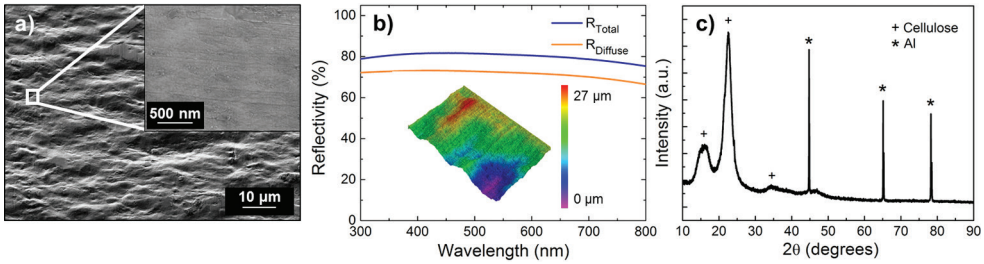

Figure 7. Surface characterization analysis of LPC. (a) SEM. Adapted from Araújo et al. [73], with permission from IOP Publishing. (b) Total and diffuse reflectivity in the visible region. The inset shows the 3D profilometer on a 3 × 2 mm area. Adapted from Vicente et al. [48], with permission from the Royal Society of Chemistry. (c) XRD diffractogram.

the cardboard and LDPE decomposition. It should also be noted that although the weight loss is negligible up to 250°C, the LDPE, responsible for the adhesion of the aluminum foil to the cardboard, starts to degrade at 200°C; thus, the substrate should be considered thermally stable up to 200°C in order to assure that the release of organic species will not influence the device fabrication.

3. Characteristics of electronic devices on paper

Although plasma-based processes, such as physical vapor deposition (PVD) and PECVD, may be relatively complicated and expensive in comparison to what is common in the graphics and printing industries (roll-to-roll), these techniques give rise to higher efficiency devices. Therefore, it is important to develop a better understanding of how these plasma processes can be applied and are influenced by paper substrates, so that a comparison can be established for the same devices produced with organic materials and printing techniques. As an example, in the more recent demonstrations of transistors on paper, there is still typically a trade-off between the transistor performance and its printability. While high-performance conventional silicon-based transistors have been attached to a silicon-coated paper substrate [34], screen printed silicon nanoparticle-based transistors on paper showed rather poor characteristics [82]. Laboratory scale techniques were also used when fabricating conventional organic field-effect transistors (OFETs) operating at high [22] or low voltages [83] on paper substrates, while simple electrochemical organic transistors operating at low voltages have been produced on polyethylene-coated paper [84] and on photo paper [85].

In this section, we provide examples of field effect transistors (FETs) fabricated on the studied substrates described in the previous section and highlight the impact cellulose has on the device properties (**Figure 8**). The transistor is one of the essential active components in electronics and its fabrication complexity makes it an ideal element to test the viability of paper electronics, and since it requires energy to operate, it is also an opportunity for solar power. In the specific case of FETs, paper is not only the support but also an active part of the device—the gate dielectric—according to the electric double layer (EDL) formation due to the mobile

http://dx.doi.org/10.5772/66695

protons within the cellulose matrix [39, 41, 86]. This cellulose role is similar to what happens in electric double-layer capacitors.

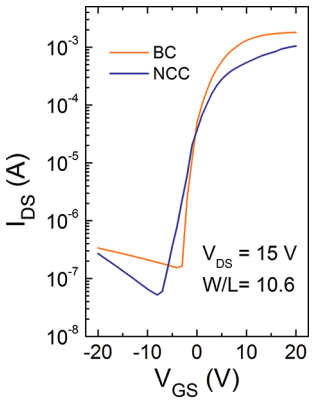

Figure 8. I_{DS}–V_{GS} transfer characteristics obtained at V_{DS} = 15 V for GIZO field effect transistors using bacterial cellulose (BC) and nanocrystalline cellulose (NCC) as gate dielectric.

The transistor fabrication comprises, on one side of the paper, a GIZO (Ga_2O_3-In_2O_3-ZnO) thin film, to create the channel region, followed by the Al e-beam evaporation of the source/drain electrodes (S/D). On the opposite side of the paper substrate, a conductive IZO (In_2O_3-ZnO) thin film is deposited by RF sputtering to work as gate electrode. To ensure the proper functioning, the devices were annealed in air for 30 min at 150°C.

The electronic performance of the BC-based FETs is similar to the FETs reported in the literature using commercial paper as dielectric, reaching a I_{ON}/I_{OFF} modulation ratio above 10^4, whereas NCC-based FETs show a saturation mobility above 7 $cm^2 V^{-1} s^{-1}$, and a I_{ON}/I_{OFF} modulation ratio higher than 10^5 [40].

The creation of the EDL depends on the mobile-free ions present in the paper matrix and fundamentally on the sorbed water within the paper. To infer the role of water content in the paper, due to humidity variations, and relate it with the performance of FETs, Fourier transform infrared (FTIR) spectroscopy was performed under normal atmosphere and in vacuum, for devices fabricated on tracing paper (TP).

In the FTIR-ATR spectra, the bands related to the adsorbed water are mainly located around 700 cm^{-1}, which corresponds to the out-of-plane vibrations of OH groups or to the rotational vibrations of H_2O molecules, whereas OH bending of adsorbed water is ascribed to the band observed at 1635 cm^{-1}. In order to assess the major differences among the samples, the spectra were normalized to the intensity of the 2900 cm^{-1} band, since it is not susceptible to variations in crystallinity or water content [69] (**Figure 9a**). The measurements taken for different vacuum times reveal that there is an abrupt decrease in intensity for the band at 1635 cm^{-1}. This observation is related to the structure compactness, whereas the more porous the structure, the more it facilitates adsorption and desorption of water.

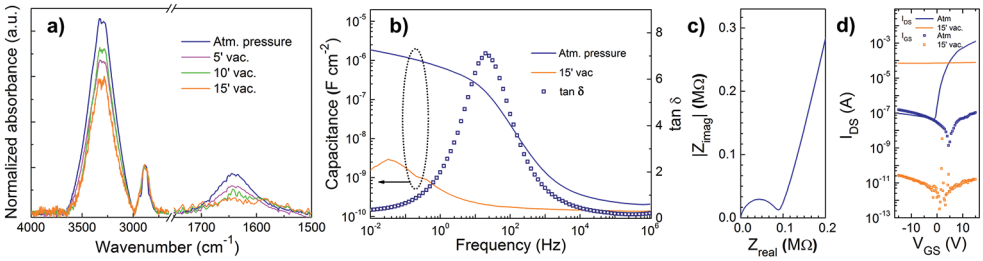

Figure 9. Correlation between electrical properties and water content variation for tracing paper (TP). (a) ATR-FTIR spectra of the water content variation (bands 3600–3000 cm^{-1} and 1635 cm^{-1}); (b) capacitance (C-f), and tan δ (tan δ-f) variation with frequency at atmospheric pressure and after 15 min of vacuum pumping; (c) high frequency region of the Cole-Cole plot; (d) transfer characteristics (V_{DS} = 15 V) of the paper gated GIZO FETs under atmospheric pressure and vacuum. Adapted from Gaspar et al. [74] Copyright Wiley-VCH Verlag GmbH & Co. KGaA. Reproduced with permission.

Water and mobile-free ions are intrinsically linked to EDL formation, when using paper as dielectric. To understand the role of ions and water, spectroscopic impedance can provide information of the paper electrical properties, namely, the capacitance variation with frequency (C-f) and bulk resistance (**Figure 9b**).

The C-f plot was determined between 10 mHz and 1 MHz using an AC excitation voltage of 500 mV [41]. In this frequency range, there is an increase in the capacitance for low frequencies, which is a typical behavior for the electrode polarization as a result of the interaction between the charged electrode surface with the free charges in the paper. For 10 mHz, the capacitance of TP is 1.8 μF cm^{-2}, and when submitted to vacuum, the capacitance decreases more than three orders of magnitude. This difference is explained by the sorbed water which is the main source of protons (H^+) and hydroxyls groups (OH^-) responsible for the behavior at lower frequencies. Drawing a parallel with FTIR-ATR results, it is possible to recognize the high susceptibility of the TP to the water variation content.

The loss tangent (tan δ) allows one to infer the relaxation frequency, by separating the contributions of the bulk material itself from the EDL regime. For high frequencies, the tan δ is low since there is no sufficient time for large dipole creation; whereas for low frequencies, the electric field action drives the ions to form the EDL, which in turn reduces tan δ [40]. The bulk resistance can also be determined from the impedance data through the Cole-Cole plot (**Figure 9c**), where the resistance of bulk material in parallel with the geometric capacitance describe a semicircle at high frequencies; the estimated resistivity for TP is 4.9 × 10^7 Ω cm. A possible explanation for this value relies in the amount of sorbed water, wherein a higher concentration can maximize the ability of free ions to migrate thought the paper matrix [41].

Regarding the other electrical properties of FETs, the saturation mobility on TP (μ_{SAT} = 2.3 cm^2 V^{-1} s^{-1}) is significantly lower compared to those fabricated on light paper (7 cm^2 V^{-1} s^{-1} for NCC).

Thus, the saturation mobility is intimately related to the density of the matrix and fraction of small fibers. The paper morphology also influences similarly the on/off current ratio (TP, $I_{on}/I_{off} = 2.5 \times 10^4$) and minimizes the gate leakage current (I_{GS}).

As for device properties, the FETs characteristics are directly affected by the decrease of water content within the paper bulk (**Figure 9d**). The susceptibility of TP to water loss, due to humidity changes, leads to no current modulation after 15 min of vacuum since the desorbed water does not allow the EDL formation. The compactness and smoothness of small fibers can give paper a higher ability to bind and retain water and ions, allowing the formation of EDLs at the interface of paper, thus enabling the semiconductor to operate under low humidity for a prolonged period [74].

4. Electrochromic devices on paper

The interest in electrochromic materials has grown from the mid-1980s, especially due to the application of these materials in smart windows for energy efficiency and indoor control [87, 88]. Nevertheless, new applications in the field of smart labels and displays have triggered the development of easier and cost-effective deposition processes that simultaneously allow patterning of the active area [89]. Inkjet printing is a good alternative for this purpose since it is processed at low temperatures, is a cost-effective technique, easily scalable for mass production, produces low waste, and can be adapted to different substrates and patterns. Nevertheless, this fabrication method can have some drawbacks as the quality of the deposited film is highly dependent on the ink characteristics, like viscosity and surface tension, combined with the printer specifications and surface properties of the paper substrate [90, 91]. So far, inkjet printed electrochromic films have been applied mostly to organic materials [92], but inorganic materials can also be easily adapted [93, 94].

An electrochemical device comprises two electrodes separated by an electrolyte, and paper can be a viable substrate to produce electrochromic displays as the next proof-of-concept shows. The electrodes are functionalized, by inkjet printing, with the electrochromic material, $WO_3 \cdot H_2O$, and at least one of the supports for the electrodes has to be fully transparent (window layer). In the case of the device shown here, liquid packaging cardboard (LPC) was used as the paper substrate and the transparent support is an ITO-coated PET substrate (for the sake of device operation and proper encapsulation), but nanocrystalline cellulose can be a viable alternative, given its high transparency and low sheet resistance of the TCOs deposited on its surface, as demonstrated by the good quality FETs fabricated on this substrate. The devices are assembled in a sandwich structure, where the ITO-coated PET/WO_3 and LPC/WO_3 are the working and counter electrodes, respectively, with the composite solid polymer electrolyte (fabricated according to Santos et al. [95]) in the middle and double-sided tape for encapsulation and spacing between electrodes. Potentiostat measurements characterize the electrochemical properties and colorimetric data studies the variations in color between different working stages.

Tungsten trioxide (WO_3) is a well-known inorganic electrochromic compound with a very high transmittance modulation, multiple oxidation states, and good cycle stability. The general reaction that describes its electrochromic behavior can be written as follows:

$$W O_3(\text{transparent/white}) + y\, M^+ + y\, e^- \Leftrightarrow M_y W O_3(\text{blue}) \quad (2)$$

The coloration occurs when the tungsten metallic center is reduced, by the application of an external potential, and a small cation ($M^+ = H^+$, Li^+, K^+,…) from the electrolyte intercalates into the material to compensate the charge insertion. The tungsten bronze (M_yWO_3) is then formed, showing the blue color in the electrode. Since this is a reversible process, when a potential with inversed polarity is applied, the reaction occurs in the opposite direction and the material returns to its initial state with a transparent/white color [89]. The full mechanism is still under discussion but the most accepted theory is explained by small polaron transitions for the amorphous material and *Drude*-like free electron scattering for crystalline. The major difference between these two mechanisms is the electron localization or delocalization:

$$W^{VI} O_3 + y\, M^+ + y\, e^- \Leftrightarrow M_y W_x^V W_{1-x}^{IV} O_3 \quad (3)$$

The x represents the number of W sites. However, at higher values of y the reaction gets irreversible and the tungsten bronze turns red or golden [96].

4.1. Liquid packaging cardboard (LPC) electrochromic device assessment

The crystallographic structure of the synthesized WO_3, analyzed by XRD (**Figure 10**), depicts a series of diffraction peaks that can be indexed to the reference pattern from the International Centre for Diffraction Data (ICDD) of the orthorhombic hydrated (or tungstic acid) WO_3 (*ortho*-$WO_3{\cdot}H_2O$) with ICDD No. 01–084–0886. Tungstic acid is already known to have a good electrochromic behavior, which is dependent on both the hydration level and crystalline structure [97, 98]. In this work, the terminal W=O and W–H_2O bonds can increase the conduc-

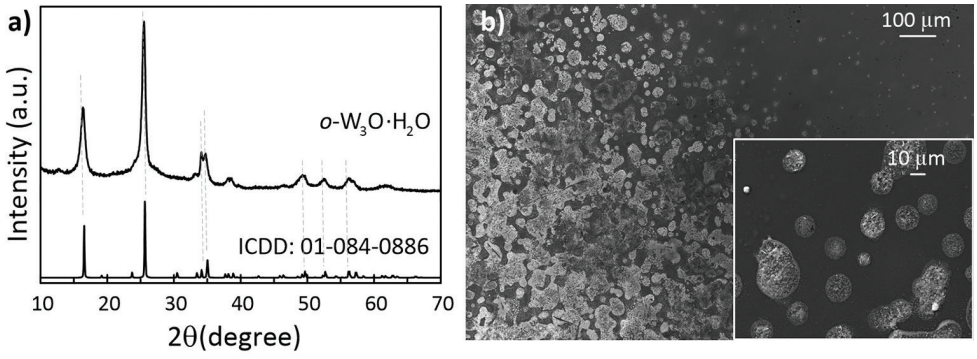

Figure 10. (a) XRD diffractogram of the $WO_3{\cdot}H_2O$ deposited film and the corresponding reference ICDD pattern. (b) SEM images of the WO_3 inkjet printed pattern detail on ITO-coated PET substrate.

tivity and diffusion of Li^+ ions, whereas the crystalline structure should improve the stability of the film [99].

The ink produced has to meet the demands of the inkjet printer used. For that, the viscosity and surface tension were between 1.5–2 cP and 30–40 dyne cm^{-1}, respectively, while the filtration assured that the nozzles would not clog during printing. As expected, the printed pattern does not show a continuous film, but the eye resolution cannot detect these irregularities [94]. The patterns were defined as a square with 1 × 1 cm for the LPC and 0.5 cm diameter circle for the ITO-coated PET substrate. This design facilitates the alignment of both electrochromic layers upon encapsulation.

Usually, the coloration of electrochromic materials is studied by UV-Vis spectroscopy; however, due to the opacity of the LPC substrate, the different colors of the device were represented by the CIE 1931 *Yxy* diagram as recommended by the *Commission Internationale de L'Eclairage*. In the CIE diagram, the quantities x and y of Eq. (3) are represented by the two Cartesian coordinates represented and are obtained by analyzing the pictures in *ImageJ* software. The x–y coordinates for each colored and bleached state are represented inside the diagram depicted in **Figure 11a**. It can be observed that there is a notable color difference between the bleached and colored states, especially at −0.6 V, where the reaction becomes irreversible. As the potential increases, the y factor in Eq. (3) also increases and the Li^+ ions become trapped in the crystalline structure of the WO_3.

The electrochemistry of the reaction studied by cyclic voltammetry (**Figure 11b**), under the same potential range (0.3 to −0.3 V and 0.6 to −0.6 V), shows that coloration occurs when the voltage and current decrease until a minimum negative value while bleaching takes place when voltage and current reach a maximum and then stabilize. In this work the capacity of the films is almost ineligible but it can be explained by the small area of the film and consequently the low amount of WO_3 material. The low current and voltage required to govern the on/off stages of the electrochromic device can be easily met by the current state-of-the-art organic [55] and inorganic [48, 49] solar cells fabricated on paper.

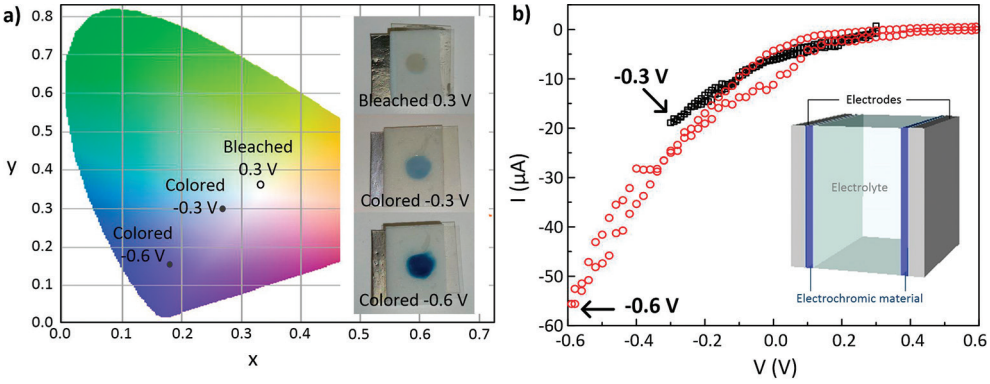

Figure 11. (a) *Yxy* chromaticity diagram for the bleached (0.3 V) and colored samples at both −0.3 and −0.6 V. (b) Cyclic voltammograms of the final devices with LPC/WO_3 and PET ITO/WO_3 electrodes in the potential ranges of 0.3 to −0.3 V and 0.6 to −0.6 V, at a scan rate of 10 and 50 mV s^{-1}, respectively. The inset illustrates the schematic representation of an electrochromic device.

5. Lab-on-paper devices

Lab-on-paper is a novel technology for fabricating simple, low-cost, portable, and disposable analytical devices holding great promise to aid global health, food quality control, and environmental monitoring [81, 100–105]. Lab-on-paper technology requires minimum fluid samples, compared to common devices, and the porous structure of the paper is solely responsible for fluid transportation. This is a crucial aspect of the diagnostic apparatus, since the substrate must facilitate the diffusion and flow of the solutions within the hydrophilic fiber matrix. The movement of fluids is governed by capillary forces, thus without the need for pumps or power [102, 103]. This technology was introduced in 2007 by Martinez et al. [106] as a method for patterning paper to create well-defined, millimeter-sized channels comprising hydrophilic paper bounded by hydrophobic polymer; but the first evidence of the lab-on-paper technology dates back to 1902 with a patent for paper strips impregnated with hydrophobic materials [107]. Earlier diagnostic applications of lab-on-paper comprise the detection of nickel and copper salt concentrations [108], determination of pH for water testing and biological analysis of urine and blood composition [109].

To date, researchers have been focused on adapting new developments in nanotechnology, biotechnology, and materials science to paper-based sensors. The production of practical analytical devices, based on those developments and by simple fabrication techniques, can have a positive impact for creating worldwide applications where they are most needed [100, 104, 106, 110, 111].

The fabrication of lab-on-paper devices starts by defining channels and reaction zones onto paper, in order to control the movement of liquids and to assure the confinement of different reagents. A wide range of diverse patterning techniques was already reported and can be divided in three major patterning principles: (i) physical blocking of pores in paper (e.g., photolithography [106], plotting [112], and laser treatment [113]); (ii) physical deposition of reagent on fiber surface (e.g., inkjet etching [114] and wax printing [104, 115]); and (iii) chemical modification of fiber surface (e.g., plasma treatment [116], inkjet printing [117], and silanization [118]). Each technique has its advantages and limitations which have to be taken under consideration according to the type of device, equipment available, material costs, and the intended application, among other factors.

5.1. Wax printing technology

Among the different patterning techniques, wax printing represents one of the most promising technology for paper patterning, given its simple and fast (5–10 min) fabrication process. The printing process uses a solid wax printer, in which the ink is supplied as solid wax and then melted, before being ejected from the print head, and once it rests on the paper surface it immediately solidifies. Since the wax remains only on the paper surface, the printed paper is then processed on a hot plate (120–140°C, 1–5 min; depending on the type of wax and paper) to allow the wax to diffuse vertically through the entire paper thickness, hence creating the hydrophobic barriers to confine the fluids (**Figure 12**). The wax is formulated from a nontoxic resin-based polymer, composed of a mixture of hydrophobic carbamates, hydrocarbons (e.g., paraffin), and dyes.

http://dx.doi.org/10.5772/66695

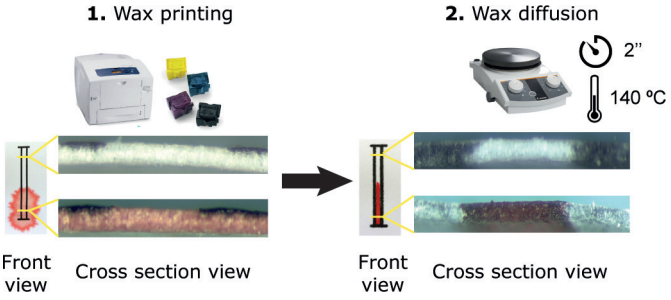

Figure 12. Schematic of the lab-on-paper technology process with wax printing: in the first step, a Xerox ColorQube printer, with solid ink (wax) cartridges, is used to print the sensor layout. The paper sheet is then processed in a hot plate (140°C, 2 min) for melting, in the second step. Digitalized images of the paper front view and the optical micrographs of the cross-section, before and after wax diffusion, show the behavior of the channel when a red dye solution is used and highlight the effect of the hydrophobic barriers. Adapted from Marques et al. [81].

5.2. Applications

The wax printing technology has already been successfully applied in the fabrication of colorimetric paper-based sensors for diagnostic and environmental applications, such as for glucose monitoring, based on enzymatic reactions [104], canine *leishmaniosis* detection through an immunoassay [104], tuberculosis detection by nucleic acid identification [100], and electrochemically active bacteria detection, based on electrochromic detection [81].

5.2.1. Glucose monitoring

Diabetes mellitus is a leading cause of illness and mortality worldwide and a major health problem for most developed societies. This metabolic disorder from insulin deficiency and hyperglycemia results in blood glucose concentrations higher or lower than the normal range (4.4–6.6 mM) [119, 120]. In developed countries where healthcare infrastructure is well established, self-monitoring of blood glucose levels is effective and economically accessible to the public. However, in many resource-limited countries the first priority is generally not given to diabetes care. Even widely used glucose meters and test strips are extremely expensive in those low-income regions; hence, there is an urgent need to develop a simple, low cost, disposable sensor that allows individuals in those countries to self-monitor their blood glucose level [121].

The work of Costa et al. [104] demonstrates how such blood glucose monitor can be fabricated on paper, as a 2D lateral flow device or as a 3D device, using the wax printing technology, for colorimetric analysis. The paper substrate used was *Whatman* filter paper n° 1 (WFP1), which is the most common paper for microfluidic devices. Briefly, the enzyme glucose oxidase (*GOx*) oxidizes glucose to D-glucono-δ-lactone and hydrogen peroxide. The enzyme peroxidase then reacts with the hydrogen peroxide and oxidizes the colorimetric indicators generating a visible color change, which is proportional to the initial amount of glucose in the sample.

Figure 13 illustrates the layers that comprise the paper-based biosensors and compares their sensibility for two different colorimetric indicators: AB (4-aminoantipyrine + 3,5-dichloro-2-hydroxy-benzenesulfonic acid) and KI (potassium iodide).

The 3D device shows important advantages compared to the 2D lateral flow sensor, given its higher coloration homogeneity. The 2D lateral flow sensor, on the other hand, is more subject to some carryover of the colored products that hinder the coloration intensity. This test runs in less than 5 min and a calibration color gradient scale can be printed directly on the paper device in order to compare with test results, allowing the patient to infer an approximate concentration of glucose in the sample. Eventually, a more complex device able to perform a wide range of analysis could take advantage of a solar cell to power sensors, a CMOS to perform logic calculations and a display to show information.

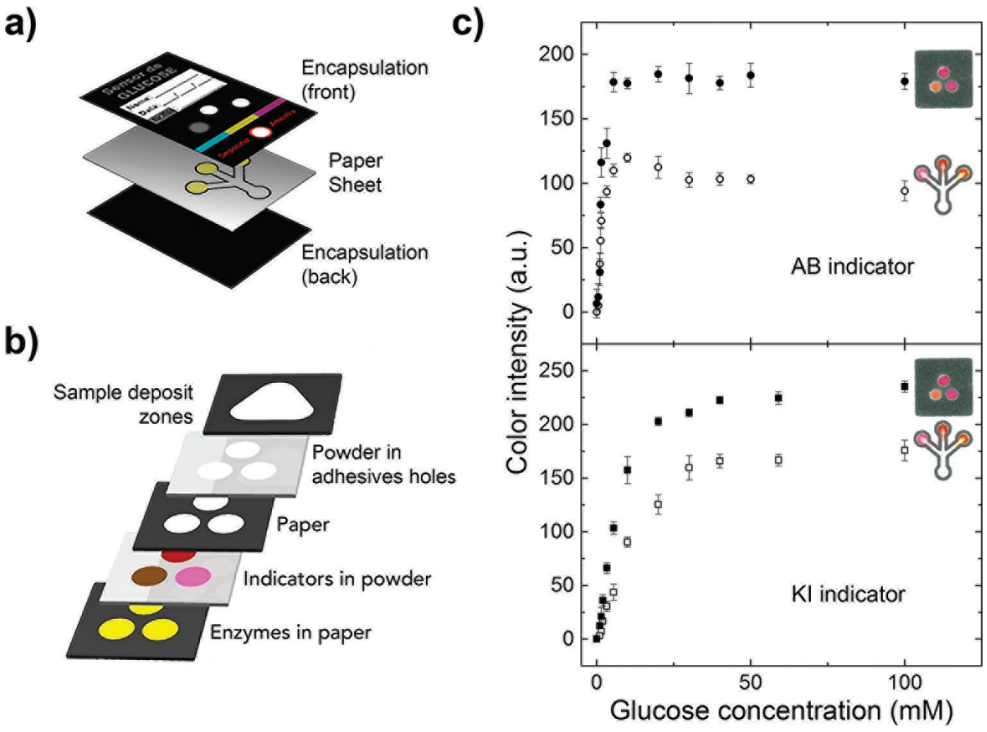

Figure 13. (a) Schematic representation of the 2D lateral flow device—enzyme and colorimetric indicators are deposited together. (b) Schematic representation of the 3D device. (c) Comparison between the 2D and 3D glucose sensors, when tested with increasing glucose concentrations (0.01–100 mM), with the graphical representations of the color intensity of detection zones containing the AB indicator (top) and the KI indicator (bottom). Adapted from Costa et al. [104], with permission from IOP Publishing.

5.2.2. Electrochemically active bacteria detection

Electrochemically active bacteria (EAB) have the ability to extracellularly transfer their electrons produced during microbial respiration [81, 122, 123]. This ability sparked interest given

http://dx.doi.org/10.5772/66695

the multiplicity of applications than can range from bioremediation to electricity production in microbial fuel cells. Although an increasing number of EAB have already been identified, isolated, and characterized, this number is still quite small regarding their ubiquity in the environment. This fact significantly constrains the fundamental knowledge about these bacteria and their role in the environment [81, 124]. To visually detect these bacteria, Marques et al. [81] developed a paper-based sensor, using common office paper (COP) as substrate and tungsten trioxide nanoparticles (WO_3 NPs) as the sensor layer (**Figure 14**), to successfully test the presence of electrochemically active *Geobacter sulfurreducens* DL-1 [125] cells (**Figure 14b**). The change in the WO_3 optical properties (between white and blue) occurs in the presence of EAB which triggers the electron-transfer (redox) process (bioelectrochromic response).

The hexagonal WO_3 NPs, hydrothermally synthesized by microwave, were integrated in a wax-printed office paper platform as an active layer for EAB detection. Common office paper allows a superficial adhesion of the WO_3 NPs, which facilitates the interaction of EAB with the electrochromic nanoparticles, promoting an intense and uniform coloration on the reaction zone, contrarily to chromatography paper (e.g., WFP).

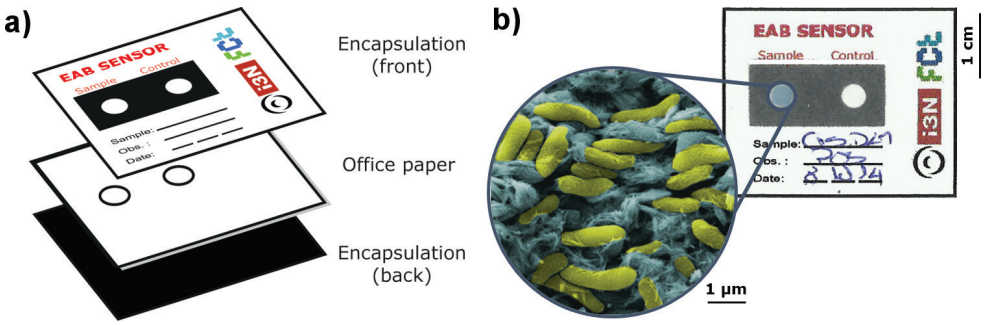

Figure 14. (a) Schematic representation of the common office paper device. (b) Digital photograph of a positive result showing a deep blue color, from the tungsten bronze, on the sample well, and nonresponse on the control well. The amplified SEM image shows the interaction between the *Geobacter sulfurreducens* bacteria (in yellow) and the hexagonal WO_3 nanoparticles (in blue). The SEM image is false-colored for better understanding of the different components. Adapted from Marques et al. [81].

6. Conclusions

Cellulose as a substrate for electronics is a highly promising booming field, not only for its low cost and recyclability, but also because of its compatibility with fast and inexpensive manufacturing printing processes. However, despite the fact that paper properties can be tuned to the intended purpose, there are still numerous challenges to address (e.g., water absorption, need for encapsulation, porosity) usually related with the internal structure, morphology, and chemistry of the fiber surface.

Unlike inorganic platforms (e.g., crystalline silicon, glass), the physical properties of paper-based materials have a considerable degree of polidispersion which can greatly affect the reproducibility of devices employing such materials. Therefore, extensive characterization protocols have to accompany the manufacturing processes, mainly targeted to provide a full

definition of the morphology and composition of the paper as they widely vary and affect immensely the properties of the electrical devices. The analysis of the different devices here described (solar cells, FETs, electrochromic displays, and lab-on-paper) highlight how certain paper substrates are appropriate in some cases, but detrimental to other devices. Nonetheless, in all cases cellulose substrates allow for working devices with similar performance to those produced on plastic or glass. These are exceptional reasons to make electronic device applications on paper a reality and encourage the progress on printed solar cells to power more complex systems such as intelligent packages or diagnostic platforms.

Acknowledgements

This work has been financed by the European Commission under projects of Horizon 2020 program BET-EU (proposal 692373), ERC Start Grant NewFun (proposal 640598), and SYMBIOTIC (proposal 665046 and 60643); the FEDER funds through the COMPETE 2020 Programme and Portuguese Science Foundation (FCT-MEC) through the Projects EXCL/CTM-NAN/0201/2012, EXPL/CTM-NAN/1184/2013, UID/CTM/50025/2013 and PTDC/CTM-ENE/5125/2014. A. T. Vicente acknowledges the support from the Portuguese Foundation for Science and Technology (FCT) and MIT-Portugal through the scholarship SFRH/BD/33978/2009. D. Gaspar acknowledges the support from AdvaMTech PhD program scholarship PD/BD/52627/2014. M. J. Mendes acknowledges support from EU FP7 Marie Curie Action (FP7- PEOPLE-2013-IEF) through the DIELECTRIC PV project (Grant No. 629370). A. Araújo acknowledges the FCT through the scholarship SFRH/BD/85587/2012. The authors want to thank their colleagues Ana Pimentel for DSC-STA measurements, Daniela Gomes for SEM images acquisition, and Rita Branquinho for helping with 3D profilometer data acquisition.

Author details

António T. Vicente*, Andreia Araújo, Diana. Gaspar, Lídia. Santos, Ana C. Marques, Manuel J. Mendes, Luís Pereira, Elvira Fortunato and Rodrigo Martins*

*Address all correspondence to: amv17109@campus.fct.unl.pt or rfpm@fct.unl.pt

CENIMAT/I3N, Department of Materials Science, Faculty of Sciences and Technology, Universidade NOVA de Lisboa and CEMOP/UNINOVA, Campus de Caparica, Caparica, Portugal

References

[1] Das R., Harrop P. Printed, Organic & Flexible Electronics Forecasts, Players & Opportunities 2016-2026. Report IDTechEx. 2016;287.

[2] Martins R., Pereira L., Fortunato E. Frontline Technology: The Future Is Paper Based. Information Display. New York, US: SID Magazine. New York, US, 2014;**30**(2):20-24.

[3] Wojcik P.J. Printable organic and inorganic materials for flexible electrochemical devices [thesis]. Universidade Nova de Lisboa - Faculdade de Ciências e Tecnologia:2013. 285 p. Available from: https://run.unl.pt/handle/10362/13600

[4] De Dobbelaere C., Calzada M.L., Jiménez R., Ricote J., Bretos I., Mullens J., et al. Aqueous solutions for low-temperature photoannealing of functional oxide films: Reaching the 400°C Si-technology integration barrier. Journal of the American Chemical Society. 2011;**133**(33):12922-12925. DOI: 10.1021/ja203553n

[5] Keszler D. Oxide electronics: Transistors pick up steam. Nature Materials. 2011;**10**(1):9-10. DOI: 10.1038/nmat2932

[6] Hardy A., Van Bael M.K. Oxide electronics: Like wildfire. Nature Materials. 2011;**10**(5):340-341. DOI: 10.1038/nmat3016

[7] George A., Stawski T.M., Unnikrishnan S., Veldhuis S. a., ten Elshof J.E. Micro and nanopatterning of functional materials on flexible plastic substrates via site-selective surface modification using oxygen plasma. Journal of Material Chemistry. 2012;**22**(2):328-332. DOI: 10.1039/C1JM14931H

[8] Banger K.K., Yamashita Y., Mori K., Peterson R.L., Leedham T., Rickard J., et al. Low-temperature, high-performance solution-processed metal oxide thin-film transistors formed by a 'sol–gel on chip' process. Nature Materials. 2011;**10**(1):45-50. DOI: 10.1038/nmat2914

[9] Kim M.-G., Kanatzidis M.G., Facchetti A., Marks T.J. Low-temperature fabrication of high-performance metal oxide thin-film electronics via combustion processing. Nature Materials. 2011;**10**(5):382-388. DOI: 10.1038/nmat3011

[10] Nomura K., Ohta H., Takagi A., Kamiya T., Hirano M., Hosono H. Room-temperature fabrication of transparent flexible thin-film transistors using amorphous oxide semiconductors. Nature. 2004;**432**(7016):488-492. DOI: 10.1038/nature03090

[11] Denneulin A., Blayo A., Bras J., Neuman C. PEDOT:PSS coating on specialty papers: Process optimization and effects of surface properties on electrical performances. Progress in Organic Coatings. 2008;**63**(1):87-91. DOI: 10.1016/j.porgcoat.2008.04.009

[12] Huebler A.C., Doetz F., Kempa H., Katz H.E., Bartzsch M., Brandt N., et al. Ring oscillator fabricated completely by means of mass-printing technologies. Organic Electronics. 2007;**8**(5):480-486. DOI: 10.1016/j.orgel.2007.02.009

[13] Khan S., Lorenzelli L., Dahiya R.S. Technologies for printing sensors and electronics over large flexible substrates: A review. IEEE Sensors Journal. 2015;**15**(6):3164-3185. DOI: 10.1109/JSEN.2014.2375203

[14] Lin Q., Huang H., Jing Y., Fu H., Chang P., Li D., et al. Flexible photovoltaic technologies. Journal of Materials Chemistry C. 2014;**2**(7):1233. DOI: 10.1039/c3tc32197e

[15] Martins R., Ferreira I., Fortunato E. Electronics with and on paper. Physica Status Solidi-Rapid Research Letters. 2011;**5**(9):332-335. DOI: 10.1002/pssr.201105247

[16] Peng B.L., Dhar N., Liu H.L., Tam K.C. Chemistry and applications of nanocrystalline cellulose and its derivatives: A nanotechnology perspective. The Canadian Journal of Chemical Engineering. 2011;**89**(5):1191-1206. DOI: 10.1002/cjce.20554

[17] Tanaka Y., Ishii N., Okuma J., Hara R. Electric double-layer capacitor having a separator made from a cellulose fiber. 1999; [Patent] US 5963419 A.

[18] Pushparaj V.L., Shaijumon M.M., Kumar A., Murugesan S., Ci L., Vajtai R., et al. Flexible energy storage devices based on nanocomposite paper. Proceedings of the National Academy of Sciences. 2007;**104**(34):13574-13577. DOI: 10.1073/pnas.0706508104

[19] Lee K.B. Two-step activation of paper batteries for high power generation: Design and fabrication of biofluid- and water-activated paper batteries. Journal of Micromechanics and Microengineering. 2006;**16**(11):2312-2317. DOI: 10.1088/0960-1317/16/11/009

[20] Nyström G., Razaq A., Strømme M., Nyholm L., Mihranyan A. Ultrafast all-polymer paper-based batteries. Nano Letters. 2009;**9**(10):3635-3639. DOI: 10.1021/nl901852h

[21] Kucherovsky J.S., Simmons G.R., Miller J.A., Mlnarik C.F. Method of making a thin film battery. 2002;**1**(12):[Patent] US 6379835 B1.

[22] Kim Y.-H., Moon D.-G., Han J.-I. Organic TFT array on a paper substrate. IEEE Electron Device Letters. 2004;**25**(10):702-704. DOI: 10.1109/LED.2004.836502

[23] Yang L., Rida A., Vyas R., Tentzeris M.M. RFID Tag and RF structures on a paper substrate using inkjet-printing technology. IEEE Transactions on Microwave Theory and Techniques. 2007;**55**(12):2894-2901. DOI: 10.1109/TMTT.2007.909886

[24] Hilder M., Winther-Jensen B., Clark N.B. Paper-based, printed zinc–air battery. Journal of Power Sources. 2009;**194**(2):1135-1141. DOI: 10.1016/j.jpowsour.2009.06.054

[25] Kim J.-Y., Park S.H., Jeong T., Bae M.J., Song S., Lee J., et al. Paper as a substrate for inorganic powder electroluminescence devices. IEEE Transactions on Electron Devices. 2010;**57**(6):1470-1474. DOI: 10.1109/TED.2010.2045675

[26] Siegel A.C., Phillips S.T., Dickey M.D., Lu N., Suo Z., Whitesides G.M. Foldable printed circuit boards on paper substrates. Advanced Functional Materials. 2010;**20**(1):28-35. DOI: 10.1002/adfm.200901363

[27] Lim W., Douglas E.A., Norton D.P., Pearton S.J., Ren F., Heo Y.-W., et al. Low-voltage indium gallium zinc oxide thin film transistors on paper substrates. Applied Physics Letters. 2010;**96**(5):053510. DOI: 10.1063/1.3309753

[28] Lu A., Dai M., Sun J., Jiang J., Wan Q. Flexible low-voltage electric-double-layer TFTs self-assembled on paper substrates. IEEE Electron Device Letters. 2011;**32**(4):518-520. DOI: 10.1109/LED.2011.2107550

[29] Irimia-Vladu M., Sariciftci N.S., Bauer S. Exotic materials for bio-organic electronics. Journal of Materials Chemistry. 2011;**21**(5):1350-1361. DOI: 10.1039/C0JM02444A

[30] Khan M.A., Bhansali U.S., Alshareef H.N. High-performance non-volatile organic ferroelectric memory on banknotes. Advanced Materials. 2012;**24**(16):2165-2170. DOI: 10.1002/adma.201200626

[31] Trnovec B., Stanel M., Hahn U., Hubler A.C., Kempa H., Sangl R., et al. Coated paper for printed electronics. Professional Papermaking. 2009;**6**:48-51.

[32] Shafizadeth F. Alternative pathways for pyrolysis of cellulose. ACS Division of Fuel Chemistry. 1983;**28**(5):285-290.

[33] Manekkathodi A., Lu M.-Y., Wang C.W., Chen L.-J. Direct growth of aligned zinc oxide nanorods on paper substrates for low-cost flexible electronics. Advanced Materials. 2010;**22**(36):4059-4063. DOI: 10.1002/adma.201001289

[34] Kim D.-H., Kim Y.-S., Wu J., Liu Z., Song J., Kim H.-S., et al. Ultrathin silicon circuits with strain-isolation layers and mesh layouts for high-performance electronics on fabric, vinyl, leather, and paper. Advanced Materials. 2009;**21**(36):3703-3707. DOI: 10.1002/adma.200900405

[35] Zocco A.T., You H., Hagen J. a, Steckl A.J. Pentacene organic thin-film transistors on flexible paper and glass substrates. Nanotechnology. 2014;**25**(9):094005. DOI: 10.1088/0957-4484/25/9/094005

[36] Bacon W.S. Now They're printing transistors on paper. Popular Science Magazine. 1968;124-125.

[37] Brody T.P. The thin film transistor - A late flowering bloom. IEEE Transactions on Electron Devices. 1984;**31**(11):1614-1628. DOI: 10.1109/T-ED.1984.21762

[38] Martins R., Ahnood A., Correia N., Pereira L., Barros R., Barquinha P., et al. Recyclable, flexible, low-power oxide electronics. Advanced Functional Materials. 2013;**23**(17):2153-2161. DOI: 10.1002/adfm.201202907

[39] Fortunato E., Correia N., Barquinha P., Pereira L., Gonçalves G., Martins R. High-performance flexible hybrid field-effect transistors based on cellulose fiber paper. IEEE Electron Device Letters. 2008;**29**(9):988-990. DOI: 10.1109/LED.2008.2001549

[40] Gaspar D., Fernandes S.N., de Oliveira A.G., Fernandes J.G., Grey P., Pontes R.V., et al. Nanocrystalline cellulose applied simultaneously as the gate dielectric and the substrate in flexible field effect transistors. Nanotechnology. 2014;**25**(9):094008. DOI: 10.1088/0957-4484/25/9/094008

[41] Pereira L., Gaspar D., Guerin D., Delattre A., Fortunato E., Martins R. The influence of fibril composition and dimension on the performance of paper gated oxide transistors. Nanotechnology. 2014;**25**(9):094007. DOI: 10.1088/0957-4484/25/9/094007

[42] Martins R., Nathan A., Barros R., Pereira L., Barquinha P., Correia N., et al. Complementary metal oxide semiconductor technology with and on paper. Advanced Materials. 2011;**23**(39):4491-4496. DOI: 10.1002/adma.201102232

[43] Tobjörk D., Österbacka R. Paper electronics. Advanced Materials. 2011;23(17):1935-1961. DOI: 10.1002/adma.201004692

[44] Zhu H., Fang Z., Preston C., Li Y., Hu L. Transparent paper: Fabrications, properties, and device applications. Energy Environmental Science. 2014;**7**(1):269-287. DOI: 10.1039/C3EE43024C

[45] Polman A., Knight M., Garnett E.C., Ehrler B., Sinke W.C. Photovoltaic materials: Present efficiencies and future challenges. Science. 2016;**352**(6283):aad4424. DOI: 10.1126/science.aad4424

[46] Ito S. Printable solar cells. Wiley Interdisciplinary Reviews: Energy and Environment. 2015;**4**(1):51-73. DOI: 10.1002/wene.112

[47] Barr M.C., Rowehl J.A., Lunt R.R., Xu J., Wang A., Boyce C.M., et al. Direct Monolithic integration of organic photovoltaic circuits on unmodified paper. Advanced Materials. 2011;**23**(31):3500-3505. DOI: 10.1002/adma.201101263

[48] Vicente A., Águas H., Mateus T., Araújo A., Lyubchyk A., Siitonen S., et al. Solar cells for self-sustainable intelligent packaging. Journal of Material Chemistry A. 2015;3(25):13226-13236. DOI: 10.1039/C5TA01752A

[49] Águas H., Mateus T., Vicente A., Gaspar D., Mendes M.J., Schmidt W.A., Pereira L., Fortunato E., Martins R. Thin film silicon photovoltaic cells on paper for flexible indoor applications. Advanced Functional Materials. 2015;**25**(23):3592-3598. DOI: 10.1002/adfm.201500636

[50] Lee C.H., Kim D.R., Cho I.S., William N., Wang Q., Zheng X. Peel-and-Stick: Fabricating thin film solar cell on universal substrates. Scientific Reports. 2012;**2**:1000. DOI: 10.1038/srep01000

[51] Lee C.H., Kim D.R., Zheng X. Transfer printing methods for flexible thin film solar cells: Basic concepts and working principles. ACS Nano. 2014;**8**(9):8746-8756. DOI: 10.1021/nn5037587

[52] Lee J., Wu J., Shi M., Yoon J., Park S.-I., Li M., et al. Stretchable GaAs Photovoltaics with designs that enable high areal coverage. Advanced Materials. 2011;**23**(8):986-991. DOI: 10.1002/adma.201003961

[53] Zhou Y., Khan T.M., Liu J.-C., Fuentes-Hernandez C., Shim J.W., Najafabadi E., et al. Efficient recyclable organic solar cells on cellulose nanocrystal substrates with a conducting polymer top electrode deposited by film-transfer lamination. Organic Electronics. 2014;**15**(3):661-666. DOI: 10.1016/j.orgel.2013.12.018

[54] Fang Z., Zhu H., Yuan Y., Ha D., Zhu S., Preston C., et al. Novel nanostructured paper with ultrahigh transparency and ultrahigh haze for solar cells. Nano Letters. 2014;**14**(2):765-773. DOI: 10.1021/nl404101p

[55] Nogi M., Karakawa M., Komoda N., Yagyu H., Nge T.T. Transparent conductive nanofiber paper for foldable solar cells. Scientific Reports. 2015;**5**:17254. DOI: 10.1038/srep17254

[56] Gao T., Wang B., Ding B., Lee J., Leu P.W. Uniform and ordered copper nanomeshes by microsphere lithography for transparent electrodes. Nano Letters. 2014;**14**(4):2105-2110. DOI: 10.1021/nl5003075

[57] van de Groep J., Spinelli P., Polman A. Transparent conducting silver nanowire networks. Nano Letters. 2012;**12**(6):3138-3144. DOI: 10.1021/nl301045a

[58] Kim W.-K., Lee S., Hee Lee D., Hee Park I., Seong Bae J., Woo Lee T., et al. Cu mesh for flexible transparent conductive electrodes. Scientific Reports. 2015;**5**:10715. DOI: 10.1038/srep10715

[59] Lyubchyk A., Vicente A., Soule B., Alves P.U., Mateus T., Mendes M.J., et al. Mapping the electrical properties of ZnO-based transparent conductive oxides grown at room temperature and improved by controlled postdeposition annealing. Advanced Electronic Materials. 2016;**2**(1):1500287. DOI: 10.1002/aelm.201500287

[60] Mendes M.J., Morawiec S., Simone F., Priolo F., Crupi I. Colloidal plasmonic back reflectors for light trapping in solar cells. Nanoscale. 2014;**6**(9):4796. DOI: 10.1039/c3nr06768h

[61] Mendes M.J., Araújo A., Vicente A., Águas H., Ferreira I., Fortunato E., et al. Design of optimized wave-optical spheroidal nanostructures for photonic-enhanced solar cells. Nano Energy. 2016;**26**:286-296. DOI: 10.1016/j.nanoen.2016.05.038

[62] Polman A., Atwater H.A. Photonic design principles for ultrahigh-efficiency photovoltaics. Nature Materials. 2012;**11**(3):174-177. DOI: 10.1038/nmat3263

[63] Ferry V.E., Verschuuren M.A., Lare M.C. Van, Schropp R.E.I., Atwater H.A., Polman A. Optimized spatial correlations for broadband light trapping nanopatterns in high efficiency ultrathin film a-Si:H Solar Cells. Nano Letters. 2011;**11**(10):4239-4245. DOI: 10.1021/nl202226r

[64] Abitbol T., Rivkin A., Cao Y., Nevo Y., Abraham E., Ben-Shalom T., et al. Nanocellulose, a tiny fiber with huge applications. Current Opinion in Biotechnology. 2016;**39**(I):76-88. DOI: 10.1016/j.copbio.2016.01.002

[65] Zhou T. Electrically conductive bacterial cellulose composite membranes produced by the incorporation of graphite nanoplatelets in pristine bacterial cellulose membranes. Express Polymer Letters. 2013;**7**(9):756-766. DOI: 10.3144/expresspolymlett.2013.73

[66] Gama M., Dourado F., Bielecki S. Bacterial nanocellulose: From biotechnology to bioeconomy. 1st ed. Oxford, UK: Elsevier, Oxford, UK; 2016. 260 p.

[67] Rojas O.J, editor. Cellulose Chemistry and Properties: Fibers, Nanocelluloses and Advanced Materials. 1st ed. Switzerland: Springer International Publishing; 2016. VII, 333 p. DOI: 10.1007/978-3-319-26015-0

[68] Gama M., Gatenholm P., Klemm D. Bacterial Nanocellulose: A Sophisticated Multifunctional Material. 1st ed. Boca Raton, Florida, US: CRC Press, Boca Raton, Florida, US; 2013. 272 p.

[69] Iguchi M., Yamanaka S., Budhiono A. Bacterial cellulose - A masterpiece of nature's arts. Journal of Materials Science. 2000;**35**(2):261-270. DOI: 10.1023/A:1004775229149

[70] Stephens C.H., Whitmore P.M., Morris H.R., Bier M.E. Hydrolysis of the amorphous cellulose in cotton-based paper. Biomacromolecules. 2008;**9**(4):1093-1099. DOI: 10.1021/bm800049w

[71] Dufresne A. Nanocellulose. From Nature to High Performance Tailored Materials. 1st ed. Berlin, Boston: De Gruyter; 2012. 460 p. DOI: 10.1515/9783110254600

[72] Stora Enso. Available from: www.storaenso.com [Accessed: June, 2016]

[73] Araújo A., Caro C., Mendes M.J., Nunes D., Fortunato E., Franco R., et al. Highly efficient nanoplasmonic SERS on cardboard packaging substrates. Nanotechnology. 2014;**25**(41):415202. DOI: 10.1088/0957-4484/25/41/415202

[74] Gaspar D., Pereira L., Delattre A., Guerin D., Fortunato E., Martins R. Engineered cellulose fibers as dielectric for oxide field effect transistors. Physica Status Solidi (c). 2015;**12**(12):1421-1426. DOI: 10.1002/pssc.201510163

[75] Ciolacu D., Ciolacu F., Popa V.I. Amorphous cellulose – Structure and characterization. Cellulose Chemistry and Technology. 2011;**45**:13-21.

[76] Łojewska J., Miśkowiec P., Łojewski T., Proniewicz L.M. Cellulose oxidative and hydrolytic degradation: In situ FTIR approach. Polymer Degradation and Stability. 2005;**88**(3):512-520. DOI: 10.1016/j.polymdegradstab.2004.12.012

[77] Segal L., Creely J.J., Martin A.E., Conrad C.M. An empirical method for estimating the degree of crystallinity of native cellulose using the X-ray diffractometer. Textile Research Journal. 1959;**29**(10):786-794. DOI: 10.1177/004051755902901003

[78] Luo Y., Zhang J., Li X., Liao C., Li X. The cellulose nanofibers for optoelectronic conversion and energy storage. Journal of Nanomaterials. 2014;**2014**:1-13. DOI: 10.1155/2014/654512

[79] Lisowski P., Zarzycki P.K. Microfluidic paper-based analytical devices (μPADs) and micro total analysis systems (μTAS): Development, applications and future trends. Chromatographia. 2013;**76**(19-20):1201-1214. DOI: 10.1007/s10337-013-2413-y

[80] Willets W, editor. Paper and Paperboard Characteristics, Nomenclature, and Significance of Tests. 3rd ed. West Conshohocken: ASTM International; 1963. 129 p. DOI: 10.1520/STP60B-EB

[81] Marques A.C., Santos L., Costa M.N., Dantas J.M., Duarte P., Gonçalves A., et al. Office paper platform for bioelectrochromic detection of electrochemically active bacteria using tungsten trioxide nanoprobes. Office Paper Platform for Bioelectrochromic Detection of Electrochemically Active Bacteria using Tungsten Trioxide Nanoprobes. 2015;**5**:9910. DOI: 10.1038/srep09910

[82] Härting M., Zhang J., Gamota D.R., Britton D.T. Fully printed silicon field effect transistors. Applied Physics Letters. 2009;**94**(19):193509. DOI: 10.1063/1.3126958

[83] Zschieschang U., Yamamoto T., Takimiya K., Kuwabara H., Ikeda M., Sekitani T., et al. Organic electronics on banknotes. Advanced Materials. 2011;**23**(5):654-658. DOI: 10.1002/adma.201003374

[84] Andersson P., Nilsson D., Svensson P.-O., Chen M., Malmström A., Remonen T., et al. Active matrix displays based on all-organic electrochemical smart pixels printed on paper. Advanced Materials. 2002;**14**(20):1460-1464. DOI: 10.1002/1521-4095(20021016)14:20<1460::AID-ADMA1460>3.0.CO;2-S

[85] Mannerbro R., Ranlöf M., Robinson N., Forchheimer R. Inkjet printed electrochemical organic electronics. Synthetic Metals. 2008;**158**(13):556-560. DOI: 10.1016/j.synthmet.2008.03.030

[86] Martins R., Barquinha P., Pereira L., Correia N., Gonçalves G., Ferreira I., et al. Write-erase and read paper memory transistor. Applied Physics Letters. 2008;**93**(20):203501. DOI: 10.1063/1.3030873

[87] Svensson J.S.E.M., Granqvist C.G. Electrochromic coatings for "smart windows". Solar Energy Materials. 1985;**12**(6):391-402. DOI: 10.1016/0165-1633(85)90033-4

[88] Svensson J.S.E.M., Granqvist C.G. Electrochromic tungsten oxide films for energy efficient windows. Solar Energy Materials. 1984;**11**(1-2):29-34. DOI: 10.1016/0165-1633(84)90025-X

[89] Mortimer R.J. Electrochromic materials. Annual Review of Materials Research. 2011;**41**(1):241-268. DOI: 10.1146/annurev-matsci-062910-100344

[90] Calvert P. Inkjet printing for materials and devices. Chemistry of Materials. 2001;**13**(10):3299-3305. DOI: 10.1021/cm0101632

[91] Hudd A. Inkjet Printing Technologies. In: Shlomo Magdassi, editor. The Chemistry of Inkjet Inks. 1st ed. Israel: World Scientific; 2009. p. 3-18. DOI: 10.1142/9789812818225_0001

[92] Shim G.H., Han M.G., Sharp-Norton J.C., Creager S.E., Foulger S.H. Inkjet-printed electrochromic devices utilizing polyaniline–silica and poly(3,4-ethylenedioxythiophene)–silica colloidal composite particles. Journal of Materials Chemistry. 2008;**18**(5):594-601. DOI: 10.1039/b712766a

[93] Wojcik P.J., Cruz A.S., Santos L., Pereira L., Martins R., Fortunato E. Microstructure control of dual-phase inkjet-printed a-WO3/TiO2/WOX films for high-performance electrochromic applications. Journal of Materials Chemistry. 2012;**22**(26):13268. DOI: 10.1039/c2jm31217d

[94] Santos L., Wojcik P., Pinto J.V., Elangovan E., Viegas J., Pereira L., et al. Structure and morphologic influence of WO3 nanoparticles on the electrochromic performance of dual-phase a-WO3/WO3 inkjet printed films. Advanced Electronic Materials. 2015;**1**(1-2):1400002. DOI: 10.1002/aelm.201400002

[95] Santos L., Nunes D., Calmeiro T., Branquinho R., Salgueiro D., Barquinha P., et al. Solvothermal synthesis of gallium–indium-zinc-oxide nanoparticles for electrolyte-gated transistors. ACS Applied Materials & Interfaces. 2015;**7**(1):638-646. DOI: 10.1021/am506814t

[96] Granqvist C.G. Oxide electrochromics: An introduction to devices and materials. Solar Energy Materials and Solar Cells. 2012;**99**:1-13. DOI: 10.1016/j.solmat.2011.08.021

[97] Choy J.-H., Kim Y.-I., Yoon J.-B., Choy S.-H. Temperature-dependent structural evolution and electrochromic properties of peroxopolytungstic acid. Journal of Materials Chemistry. 2001;**11**(5):1506-1513. DOI: 10.1039/b009119g

[98] Leftheriotis G., Papaefthimiou S., Yianoulis P. The effect of water on the electrochromic properties of WO3 films prepared by vacuum and chemical methods. Solar Energy Materials and Solar Cells. 2004;**83**(1):115-124. DOI: 10.1016/j.solmat.2004.02.019

[99] Yang J., Jiao L., Zhao Q., Wang Q., Gao H., Huan Q., et al. Facile preparation and electrochemical properties of hierarchical chrysanthemum-like WO3·0.33H2O. Journal of Materials Chemistry. 2012;**22**(9):3699-3701. DOI: 10.1039/c2jm15837j

[100] Veigas B., Jacob J.M., Costa M.N., Santos D.S., Viveiros M., Inácio J., et al. Gold on paper–paper platform for Au-nanoprobe TB detection. Lab on a Chip. 2012;**12**(22):4802-4808. DOI: 10.1039/c2lc40739f

[101] Li X., Ballerini D.R., Shen W. A perspective on paper-based microfluidics: Current status and future trends. Biomicrofluidics. 2012;**6**(1):011301. DOI: 10.1063/1.3687398

[102] Zhao W., van der Berg A. Lab on paper. Lab on a Chip. 2008;**8**(12):1988-1991. DOI: 10.1039/b814043j

[103] Liana D.D., Raguse B., Gooding J.J., Chow E. Recent advances in paper-based sensors. Sensors. 2012;**12**(12):11505-11526. DOI: 10.3390/s120911505

[104] Costa M.N., Veigas B., Jacob J.M., Santos D.S., Gomes J., Baptista P.V., et al. A low cost, safe, disposable, rapid and self-sustainable paper-based platform for diagnostic testing: Lab-on-paper. Nanotechnology. 2014;**25**(9):094006. DOI: 10.1088/0957-4484/25/9/094006

[105] Zhou M., Yang M., Zhou F. Paper based colorimetric biosensing platform utilizing cross-linked siloxane as probe. Biosensors and Bioelectronics. 2014;**55**:39-43. DOI: 10.1016/j.bios.2013.11.065

[106] Martinez A.W., Phillips S.T., Butte M.J., Whitesides G.M. Patterned paper as a platform for inexpensive, low-volume, portable bioassays. Angewandte Chemie International Edition. 2007;**46**(8):1318-1320. DOI: 10.1002/anie.200603817

[107] Dieterich K. Testing-paper and method of making same. 1902; [Patent] US 691249 A.

[108] Yagoda H. Applications of confined spot tests in analytical chemistry: Preliminary paper. Industrial & Engineering Chemistry Analytical Edition. 1937;**9**(2):79-82. DOI: 10.1021/ac50106a012

[109] Johnson J.L. Microchemical techniques in solving industrial problems. Mikrochimica Acta. 1967;**55**(4):756-762. DOI: 10.1007/BF01224400

[110] Pelton R. Bioactive paper provides a low-cost platform for diagnostics. Trends in Analytical Chemistry. 2009;**28**(8):925-942. DOI: 10.1016/j.trac.2009.05.005

[111] Jokerst J.C., Adkins J.A., Bisha B., Mentele M.M., Goodridge L.D., Henry C.S. Development of a paper-based analytical device for colorimetric detection of select foodborne pathogens. Analytical Chemistry. 2012;**84**(6):2900-2907. DOI: http://pubs.acs.org/doi/abs/10.1021/ac203466y

[112] Bruzewicz D.A., Reches M., Whitesides G.M. Low-cost printing of poly(dimethylsiloxane) barriers to define microchannels in paper. Analytical Chemistry. 2008;**80**(9):3387-3392. DOI: 10.1021/ac702605a

[113] Martinez A.W., Phillips S.T., Whitesides G.M., Carrilho E. Diagnostics for the developing world: Microfluidic paper-based analytical devices. Analytical Chemistry. 2010;**82**(1):3-10. DOI: 10.1021/ac9013989

[114] Martinez A.W., Phillips S.T., Carrilho E., Thomas S.W., Sindi H., Whitesides G.M. Simple telemedicine for developing regions: Camera phones and paper-based microfluidic devices for real-time, off-site diagnosis. Analytical Chemistry. 2008;**80**(10):3699-3707. DOI: 10.1021/ac800112r

[115] Carrilho E., Martinez A.W., Whitesides G.M. Understanding wax printing: A simple micropatterning process for paper-based microfluidics. Analytical Chemistry. 2009;**81**(16):7091-7095. DOI: 10.1021/ac901071p

[116] Li X., Tian J., Nguyen T., Shen W. Paper-Based Microfluidic Devices by Plasma Treatment. Analytical Chemistry. 2008;**80**(23):9131-9134. DOI: 10.1021/ac801729t

[117] Khan M.S., Fon D., Li X., Tian J., Forsythe J., Garnier G., et al. Biosurface engineering through ink jet printing. Colloids and Surfaces B: Biointerfaces. 2010;**75**(2):441-447. DOI: 10.1016/j.colsurfb.2009.09.032

[118] Glavan A.C., Martinez R.V., Subramaniam A.B., Yoon H.J., Nunes R.M.D., Lange H., et al. Omniphobic "RF Paper" produced by silanization of paper with fluoroalkyltrichlorosilanes. Advanced Functional Materials. 2014;**24**(1):60-70. DOI: 10.1002/adfm.201300780

[119] Wang J. Electrochemical glucose biosensors. Chemical Reviews. 2008;**108**(2):814-825. DOI: 10.1021/cr068123a

[120] Yoo E.-H., Lee S.-Y. Glucose biosensors: An overview of use in clinical practice. Sensors. 2010;**10**(5):4558-4576. DOI: 10.3390/s100504558

[121] Fischer C., Fraiwan A., Choi S. A 3D paper-based enzymatic fuel cell for self-powered, low-cost glucose monitoring. Biosensors and Bioelectronics. 2016;**79**:193-197. DOI: 10.1016/j.bios.2015.12.020

[122] Lovley D.R. Bug juice: Harvesting electricity with microorganisms. Nature Reviews Microbiology. 2006;**4**(7):497-508. DOI: 10.1038/nrmicro1442

[123] Lovley D.R. The microbe electric: Conversion of organic matter to electricity. Current Opinion in Biotechnology. 2008;**19**(6):564-571. DOI: 10.1016/j.copbio.2008.10.005

[124] Yuan S.-J., He H., Sheng G.-P., Chen J.-J., Tong Z.-H., Cheng Y.-Y., et al. A Photometric high-throughput method for identification of electrochemically active bacteria using a WO3 nanocluster probe. Scientific Reports. 2013;**3**:1315. DOI: 10.1038/srep01315

[125] Lovley D.R., Ueki T., Zhang T., Malvankar N.S., Shrestha P.M., Flanagan K.A., et al. Geobacter: The Microbe Electric's Physiology, Ecology, and Practical Applications. In: Poole R.K., editor. Advances in Microbial Physiology. 1st ed. United Kingdom: Elsevier; 2011. p. 1-100. DOI: 10.1016/B978-0-12-387661-4.00004-5